Journal of Materials Chemistry C

ROYAL SOCIETY OF CHEMISTRY

PAPER

View Article Online
View Journal | View Issue

Cite this: J. Mater. Chem. C, 2023, 11, 5199

Irradiation-responsive polysulfone film as a colorimetric UVA/UVB differentiator†

Bernardo Monteiro,[a] João Paulo Leal,[b] Mani Outis,[c] Maria Helena Casimiro[d] and Cláudia C. L. Pereira *[c]

Received 3rd March 2023,
Accepted 28th March 2023

DOI: 10.1039/d3tc00782k

rsc.li/materials-c

A wearable, small size, flexible and energy consumable free colorimetric detector of UVA radiation and UVB/UVA differentiation was created based on the peculiar stimuli-responsive behaviour of an imidazolium based ionic liquid. Semi-transparent polysulfone films are transformed into opaque and homogenous red films under UVA radiation (315–360 nm), while lower wavelength exposure (280–315 nm) induces increased emission detectable under dark light, with no colour modification of the film under visible light. Thermal analysis (TGA and DSC), spectroscopic analysis (FT-IR, ^{1}H-NMR and UV-Vis), scanning electronic microscopy (SEM) and energy dispersive X-ray spectroscopy (EDS) were conducted to elucidate confinement mechanism and irradiation effects.

1. Introduction

Significant health problems such as skin aging, sunburn (erythema), skin cancer or eye diseases, can result from exposure to sunlight for long periods. Electronic UV dosimeters use a wide band gap aluminium gallium nitride (Allegan) Schottky photodiode as the key UV sensing element, that produces a photocurrent in the nanoampere range when exposed to UV solar light.[1,2] This type of equipment is usually bulky and requires individual calibration and maximum alignment with the incoming light, which renders them less adequate as wearable devices. Epidermis and dermis tolerance to UV radiation is higher in dark skin types, so personalised dosimeters will monitor more adequately the risk of a certain dose of exposure.

For a detailed explanation of relating UV and UV-Index, which is the widely accepted and commonly known standard that indicates the risk of skin damage, the authors suggest several articles where they are discussed and related.[3–6]

Wearable technologies are an alternative, and incorporation of UV-sensitive dyes in polymeric matrices has been an excellent approach, although facing challenges, that include stability over a wide range of temperatures, dye protection from oxygen degradation and the need of significant flexibility and miniaturization.

Recently a modified flexible poly(methyl acrylate) film was prepared using the photocleavable ortho-nitrobenzyl (ONB) that irreversibly cleaves and changes colour upon exposure to UV light.[7] Jokerst *et al.* published in 2018 a film dosimeter made of a purple photodegradable dye blended in low density polyethylene film that degrades from purple to colourless upon cumulative UV exposure.[8]

Polysulfone (PSU) is a polymer with excellent mechanical, thermal and processable properties, and has fine film-forming characteristics. In terms of fluorescence, PSU absorbs light close to 340 nm and emits an Indigo-blue fluorescence at 380 nm.[9]

The potential use of PSU as dosimeter for measuring solar UV radiation was studied by A. Davis, B. L. Diffey and G. H. W. Dean after detecting film darkening under ultraviolet radiation, attributed to degradation and loss of tensile properties.[10] Simultaneously, the broad absorption band in the near ultraviolet, extended to visible, with increment relatable with the incident ultraviolet dose. The small size of PSU based film dosimeters allows them to be particularly suited to measure the anatomical distribution of solar UV radiation, as reported in a study, the level of exposure around the eyes.[11] B. Diffey[12] and J. K. Vanos[13] recently published a detailed revision of PSU and other wearable films used for UV dosimetry.

From the above presented PSU photochromic properties, in combination with the unusual photochromism of a new imidazolium based ionic liquid we developed a flexible and

[a] Centro de Química Estrutural (CQE), Departamento de Engenharia Química (DEQ), Instituto Superior Técnico, Universidade de Lisboa, Campus Tecnológico e Nuclear, Estrada Nacional 10, Bobadela 2695-066, Portugal
[b] Centro de Química Estrutural (CQE), Departamento de Engenharia e Ciências Nucleares (DECN), Instituto Superior Técnico, Universidade de Lisboa, Campus Tecnológico e Nuclear, Estrada Nacional 10, Bobadela 2695-066, Portugal
[c] LAQV-REQUIMTE, Departamento de Química, Faculdade de Ciências e Tecnologia, Universidade Nova de Lisboa, Caparica 2829-516, Portugal. E-mail: ccl.pereira@fct.unl.pt
[d] Centro de Ciências e Tecnologias Nucleares (C^{2}TN), Instituto Superior Técnico, Universidade de Lisboa, Campus Tecnológico e Nuclear, Estrada Nacional 10, Bobadela, 2695-066, Portugal

† Electronic supplementary information (ESI) available. See DOI: https://doi.org/10.1039/d3tc00782k

semi-transparent film with outstanding and rarely observed selective response toward UVA and UVB radiation.

The immobilization of ILs in several type of polymers creates the opportunity of developing multifunctional membranes, films, fibres, and porous coordination polymers (PSPs) with stimuli-responsive properties.[14–16]

In our system, light irradiation induces a modification in the polymer film, resulting in a change of the emission intensity and excitation spectra. In this study, from the combination between the PSU photochromic properties with the unusual photochromism of a new imidazolium based ionic liquid with a highly fluorinated β-diketonate as counter-anion, [C_2mim][fod] (C_2mim = 1-ethyl-3-methylimidazolium, fod = 1,1,1,2,2,3,3-heptafluoro-7,7-dimethyl-4,6-octanedionate), we developed a flexible and semi-transparent film with outstanding and rarely observed selective response toward UVA and UVB radiation.

Both UVA and UVB induce skin cancer; UVA has a longer wavelength and is associated with skin aging, while UVB is associated with skin burning. Although less intense, UVA penetrates deeper in your skin and are also able to cross windows and cloudy weather, maintaining the same level of strength during daylight throughout the year. For this reason, it is important to distinguish the exposure to UVA, independently of the presence of UVB radiation.

Nowadays, there are thirteen wearable UV sensors commercially available for personal use and/or research applications. These present large differences in price, precision, accuracy, types of data outputs that vary from photochromic to electronic and were recently reviewed.[13]

In this work we propose a photochromic membrane, [C_2mim][fod]@PSU, for fast and real-time detection and differentiation of UVA and/or UVB radiation (Fig. 1).

2. Results and discussion

The Results and Discussion section is organised as follows; photophysical properties of the guest ([C_2mim][fod]), the photophysical properties of the host–guest systems, the detailed discussion of Scanning Electron Microscopy (SEM) of the PSU dopped films and finally water contact angle determination to evaluate the hydrophobic character of the pristine and irradiated films.

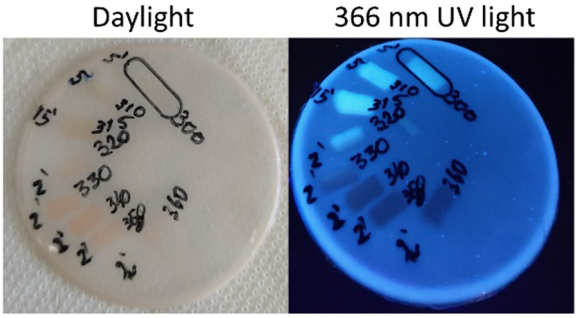

Fig. 1 Pictures of the here presented doped PSU film after irradiation at different wavelengths (300–360 nm, on the right) and time of exposure (2, 5 and 15 min, on the left).

Previous work has demonstrated thermochromism of highly fluorinated β-diketonate lanthanide based ionic liquids, with reversible colour change from light yellow to red upon heating at 80 °C.[17] Despite the presence of reversible thermochromism, our focus in this research work was on the photochromic properties of the here presented IL and when embedded in a polysulfone film. Briefly, [C_2mim][fod] is prepared through simple ion exchange between C_2mimCl or C_2mimBF_4 and deprotonated Hfod. Synthetic details and chemical characterization are described in ESI.†

Electrospray ionisation mass spectrometry (ESI/MS) revealed the presence of supramolecular cationic and anionic aggregates, which gives indication of considerable strength of anion-cation interaction (Fig. S1 and S2, ESI†).

Thermal stability was determined by thermogravimetric analysis. TGA curve of the as-synthesized and irradiated [C_2mim][fod] has an initial weight loss before 100 °C, which can be assigned to the release of organic solvent molecules. As shown (Fig. S3, ESI†) [C_2mim][fod] starts to decompose near 250 °C, when the organic moieties degrade, presenting a mass loss of 65%. The next step represents 15% of mass loss where only non-volatile residues are formed, typical of highly fluorinated organic compounds.[18]

Phase transition was evaluated by differential scanning calorimetry (DSC) (Fig. S4, ESI†) and shows an experimental melting temperature of 66.7 °C (T_{on} = 61.1 °C) with a ΔH of 12.4 kJ mol^{-1} and a solidification temperature of 62.3 °C (T_{on} = 63.2 °C) with a ΔH equal to 12.5 kJ mol^{-1}.

2.1 Photochromism of [C_2mim][fod] ionic liquid

[C_2mim][fod] is a white solid that if irradiated with UV light above 310 nm has a distinct colour change to red (Fig. 2).

Changes in the ^{1}H-NMR spectra were reported after UV light irradiation of an imidazolium DAEs-PIL (diarylethene based polymeric ionic liquids) in the solid state.[19] It was concluded that irradiation induces electron redistribution in the imidazolium ring with significant upfield shift in the proton at C2 position.

^{1}H-NMR analysis of post irradiated solid (Fig. S5, ESI†) only revealed upfield shift in the acidic H_α of fod$^-$ anion (Fig. 3). With this information we suggest that increased interaction between anion and cation induced a shielding effect in H_α provided by imidazolium aromatic electrons.

The spectroscopic characteristics of this new highly fluorinated imidazolium ionic liquid, in is neat form are illustrated in Fig. 4. Ionic liquids with [C_nMIM] cations are expected to be transparent in the visible range, with absorption band maximum falling into

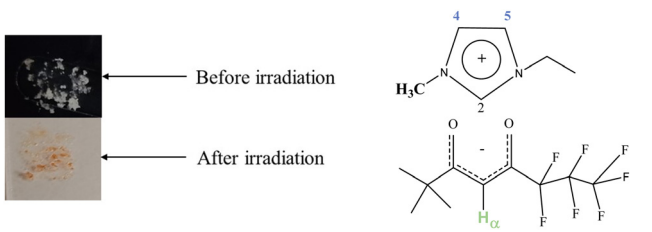

Fig. 2 [C_2mim][fod] before and after irradiation at 310 nm (left) chemical structure of [C_2mim][fod] (right).

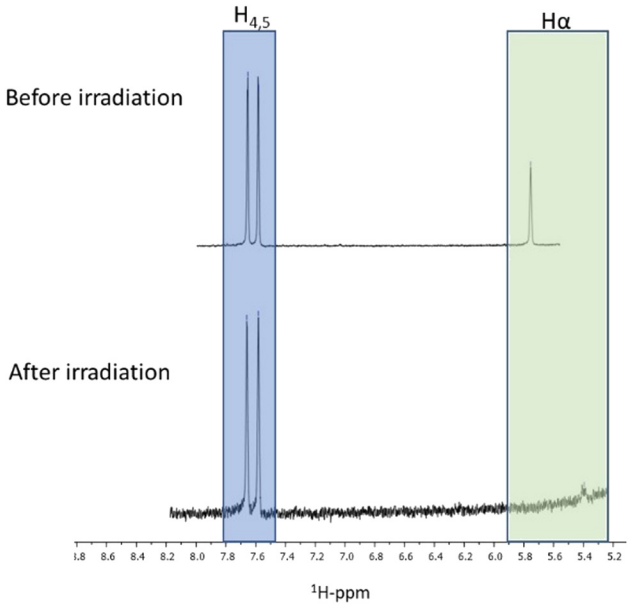

Fig. 3 ^{1}H-NMR overlay spectra of [C_2mim][fod] before and after irradiation at 340 nm in methanol-d.

the UV region due to the $\pi \rightarrow \pi^*$ transition from the C=C bond of the imidazolium cation.[20,21] A very weak and broad green light emission around 475 nm is observed and eventually comes from dimerization of imidazole after imidazolium cation deprotonation in which the most acidic proton is deprotonated to yield a neutral carbon atom with lone-pair electrons that is known for being highly reactive towards imidazole formation.[22] Generally the emission intensity is very weak, with maximum at 360 nm after excitation at 310 nm.

2.2 Photophysical properties of host–guest systems under irradiation

As aforementioned, polysulfone film dosimeters respond to short UVA and UVB wavelengths from 254 to 335 nm by degrading and experiencing a colour change when exposed to UV light.[10] Also, these films have increased absorbance at 330 nm upon receiving cumulative UV radiation,[23] although characteristic PSU emissive intensity decreases when exposed to 335 nm. Using this feature, we impregnated polysulfone polymer with [C_2mim][fod], above described with photochromic properties when exposed to UV radiation.

The originality of these results comes from the modification of the fluorescence spectra intensity, upon irradiation, that is also excitation wavelength dependent.

The excitation spectra of the host–guest film, [C_2mim][fod]@PSU have two well separated maximum peaks, at 293 nm and at 340 nm (Fig. 5).

The films were easily prepared by physically blending the photo-responsive molecule in the polymer matrix. They are easily bended suggesting considerable flexibility, with a semi-transparent aspect with 7% (w/w) of [C_2mim][fod] impregnated in the polymer. Visual examination of the hybrid materials reveals that the samples are fully continuous and homogenous along the entire film (Fig. 6 inset). The transparency was evaluated by UV-vis spectroscopy, by measuring the transmittance in the visible domain, at room temperature. The transmittance of the dopped film was close to 55% at 800 nm and decreased drastically over the visible light region, with minimum value of 10% at 400 nm. Opacity, is a figure of merit that correlates better the 'see through' property and is defined as:

$$\text{Opacity} = A_{600}/x$$

where A_{600} is the absorbance of light at 600 nm and x is the thickness of the film.[24]

The opacity of the prepared film was 8.4 mm^{-1}.

After short periods of continuous excitation wavelength exposure, the intensity of the emission band centred at 390 nm increased 83% upon irradiation at 293 nm, to which corresponds a total period of 2 minutes of light exposure. Conversely, excitation at 340 nm induced a significant decrease of emission intensity and equal to 66%. The irreversibility of

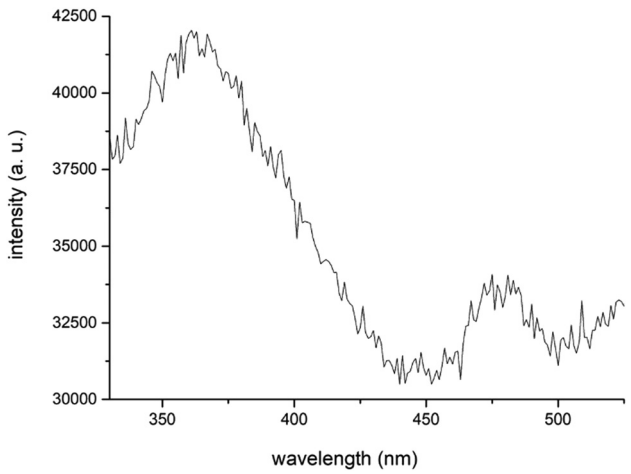

Fig. 4 Emission spectra of [C_2mim][fod] with excitation wavelength at 310 nm.

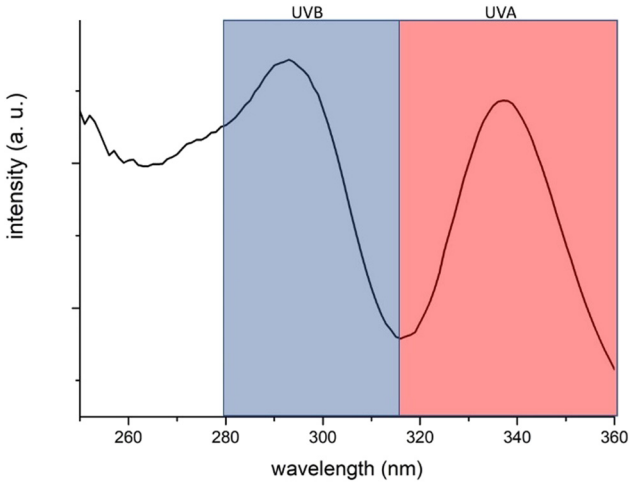

Fig. 5 Excitation spectra of [C_2mim][fod] @PSU for the maximum emission band at 390 nm.

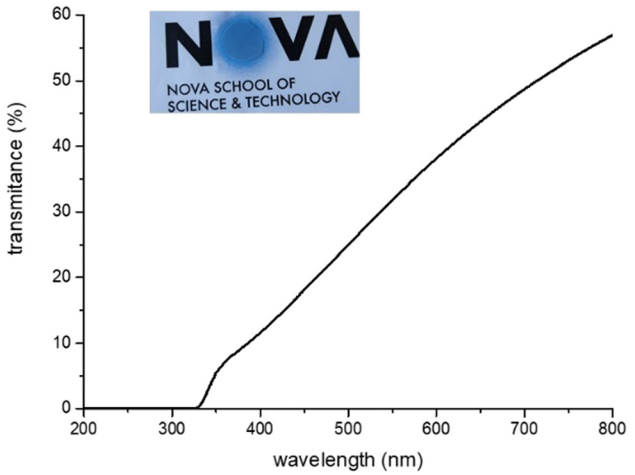

Fig. 6 Transmittance of PSU film doped with 7% of photoactive [C_2mim][fod] with 50 μm thickness. Inset: Picture of the prepared film covering the blue spot.

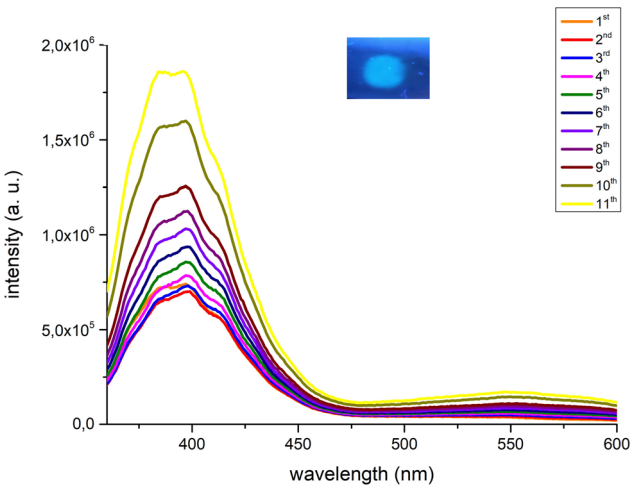

Fig. 8 Emission spectra of eleven consecutive acquisitions of [C_2mim][fod]@PSU film with excitation wavelength of 290 nm. Inset indicates the irradiated area.

the emissive properties of the films was unexpected and opposite to what is published in literature relative to other polymeric doped films.[19,25] Instead, PSU film degradation starts, before the detection of any reversible process.

The dopped PSU film works as follows; under exclusive UVA radiation (315–360 nm) the film colour evolves from white opaque to red, under exclusive UVB radiation (280–315 nm) the colour of the film is maintained, and the irradiated section emits more intensively in the blue region when observed under dark light (366 nm) (Fig. 7). If both UVA and UVB are present in the irradiation source, the film will evolve to red, which is detected by naked eye and simultaneously, under the same irradiated area, it will emit brighter when observed under a 366 nm UV lamp.

2.2.1 Irradiation at 290 nm of [C_2mim][fod]@PSU. The emission spectrum is composed by a broad band ranging from 360 to 450 nm ascribed to polysulfone inherent fluorescence. Fig. 8 shows the emission spectra of successive spectral acquisitions of the dopped PSU film using one of the most intense maximum excitation wavelengths (λ_{exc} 290 nm). No visual modifications were detected on the film after irradiation for short periods, which indicates some resistance to degradation under UVB exposure. The increased emission intensity can be seen by illuminating with a 366 nm UV lamp, when the weak bluish luminescence characteristic of pristine PSU becomes shining (inset Fig. 8).

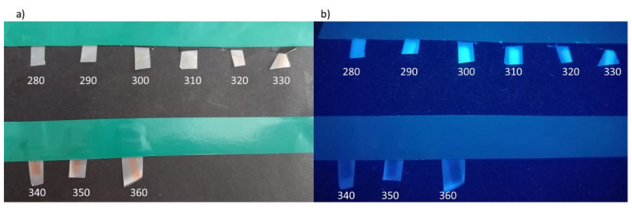

Fig. 7 [C_2mim][fod]@PSU film irradiated with 10 nm step between 280 and 360 nm. (a) Under daylight, (b) under 366 nm UV lamp.

Interestingly, upon irradiation the excitation spectra changed in intensity and shape. The irradiation-dependent excitation spectra presented broader and more intense bands, with maximum wavelength between 300 and 330 nm (Fig. 9).

The quantum yield (φ), which is defined as the ratio between the number of emitted and absorbed photons, was determined by the integrating sphere method for the hybrid material after irradiation at 290 nm. The irradiated film presented an emission quantum yield of 2.3%, significantly higher than the non-irradiated film ($\sim$0%), which may indicate a more efficient intermolecular energy transfer after exposure to UV at the lowest wavelength.

2.2.2 Irradiation at 340 nm of [C_2mim][fod]@PSU. Irradiation at 340 nm, one of the most intense excitation bands of the dopped film, induced decreased emission intensity (Fig. 10) with simultaneous coloration of the film from light white opaque to red.

This interesting photochromic behaviour is probably related with the above discussed effect of irradiation of [C_2mim][fod], that is comparable with the thermochromism already reported for several salts based on the here reported fluorinated β-diketone.

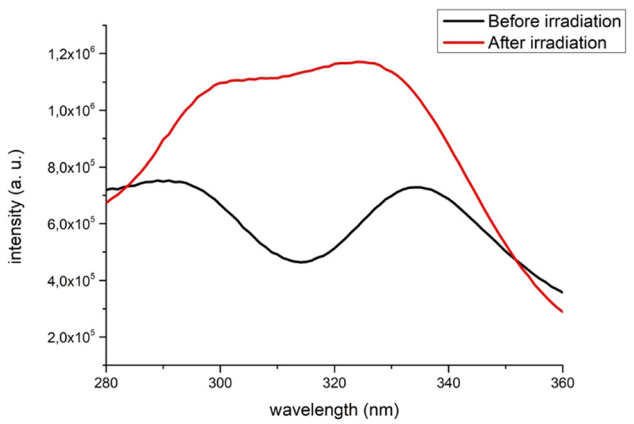

Fig. 9 Excitation spectra before and after successive irradiation of [C_2mim][fod]@PSU at 290 nm.

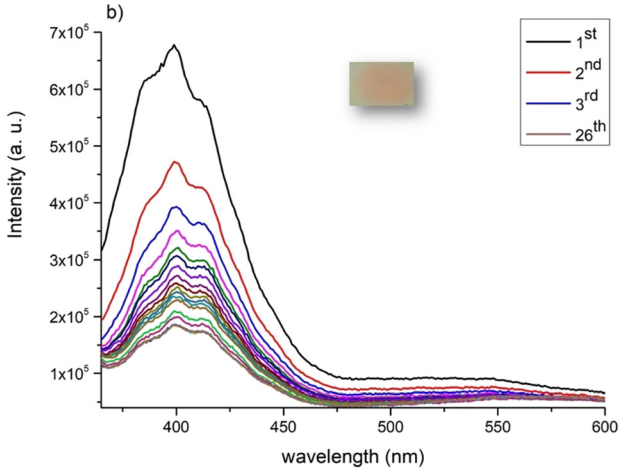

Fig. 10 Emission spectra of 26 consecutive acquisitions (1st–26th) of [C_2mim][fod]@PSU film with excitation wavelength of 340 nm. Inset indicates the irradiated area.

2.2.3 Irradiation of pristine PSU and other guests immobilized in PSU. Due to lack of conclusive evidence regarding the mechanism associated with this interesting and unusual photochromism, doped PSU films were prepared with reagents involved in the preparation of [C_2mim][fod]. All polysulfone films embedded with reaction precursors, Nafod, [C_2mim][BF_4] and [C_2mim][Cl], show emissive properties, surprisingly, with a very peculiar behaviour after successive irradiations at each guest maximum excitation wavelengths. These compounds were used as guests in PSU in an attempt to clarify the unexplained increased emission intensity of [C_2mim][fod]@PSU upon irradiation at 290 nm.

In 2015 Nakamura *et al.* reported the emission of a Indigo-blue light of a dense PSU film, with maximum emission spectra at 380 nm when excited at 340 nm maximum.[9] Despite this observation, the first dose-response curve, was obtained after irradiation at 297 ± 5 nm.[12] A careful analysis of excitation spectra of PSU shows a low intense band at close 295 nm, together with the expected intense excitation band at 325 nm (Fig. S6, ESI†). Irradiation of a thin film of PSU at 295 nm also induces increased emission until reaching a plateau after only five acquisitions (Fig. 11a); while irradiation at 325 nm, correspondent to the most intense excitation band, no modification of emission band intensity was observed (Fig. 11b).

Surprisingly, and as far as we know, this behaviour has never been reported in literature but is probably related with the increased emissive properties of impregnated PSU films when exposed to lower wavelength (280–310 nm). One hypothesis, that was already raised by Elena Perju and co-workers in doped azomethine core PSU films, refer to the possibility of restricting intramolecular rotation, reducing nonradiative channels and photoluminescence intensity enhancement, with a significant red-shift of the emission maximum.[26] For pristine PSU we observed a red-shift of 10 nm after irradiation at 295 nm for some minutes.

In morphological terms, Scanning Electron Microscopy (SEM) revealed identical surface images and composition between PSU and 295 nm irradiated PSU, while irradiation at 325 nm increased the heterogeneity of the film, with some irregular spots with unaltered chemical composition relative to other PSU films (Fig. S7, ESI†).

Ultraviolet radiation is frequently used in curing processes of membrane preparation. This process increases crosslinking of several small polymer units, even when very short periods of UV radiation are used.[27] We suggest that radiation at 295 nm could have promoted crosslinking of free monomeric units, increasing the PSU inherent emissive characteristics.

Other interesting results were obtained after embedding [C_2mim][fod] starting reagents; Nafod, and [C_2mim][BF_4]. The film doped with Nafod presented very similar excitation spectra with the one correspondent to [C_2mim][fod]@PSU, with two distinct intense bands at 295 and 335 nm. (Fig. S8, ESI†), while [C_2mim][BF_4]@PSU presented only broad excitation band with maximum at 315 nm (Fig. S9, ESI†). From this observation we can conclude that the highly fluorinated β-diketonate anion has a relevant and unique role for the contribution of two intense excitation wavelengths in the doped film, while [C_2mim][BF_4] only contributes with one intense excitation wavelength.

2.3 Scanning electron microscopy and energy dispersive X-ray spectroscopy

Surface features were evaluated by Scanning Electron Microscopy (SEM), including matrix homogeneity, surface smoothness of the

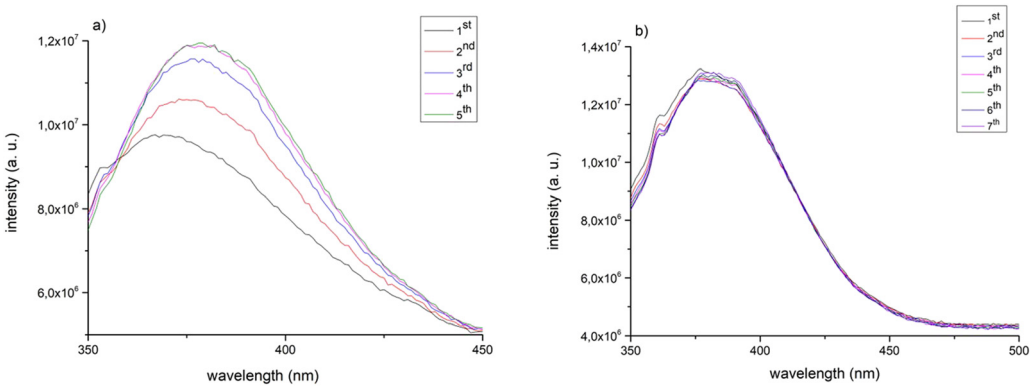

Fig. 11 (a) Emission spectra of pristine PSU film upon successive irradiations (1st–5th) at 305 nm. (b) Emission spectra of pristine PSU film upon irradiation at its maximum excitation wavelength, 325 nm upon successive irradiations (1st–7th).

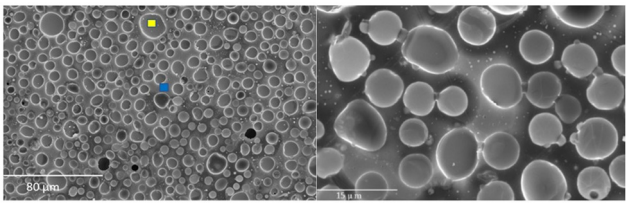

Fig. 12 Morphology of [C_2mim][fod]@PSU with 7% loading with agglomerates (yellow square) with spherical shape and film background in the blue square (left image). Magnification showing neck-shaped bonds between the drops (right image).

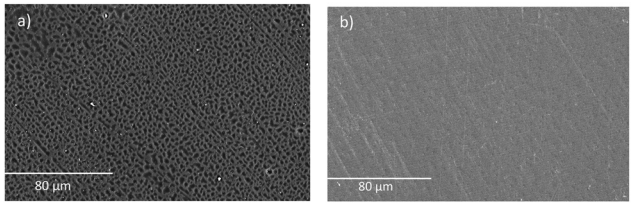

Fig. 13 SEM images of [C_2mim][fod]@PSU after irradiation at (a) 290 nm (b) 340 nm.

PSU film (Fig. S10, ESI†) and surface modification of the immobilized material after irradiation at 290 and 340 nm. As expected, pure PSU film exhibited a dense structure with a relatively smooth and even surface.

SEM images of [C_2mim][fod]@PSU (Fig. 12) show two distinct domains including aggregated structures with spherical morphology with maximum size of 17 µm. Irradiation at 290 nm induced formation of particles with lower dimensions and close to 3 µm (Fig. 12a), while fibrillar form with 100 µm size (Fig. 12b) where found after irradiation at higher wavelength, which are also characteristic of other highly fluorinated imidazolium salts when embedded in polyvinyl acrylate matrix.[28] Therefore, irradiation affected significantly the size and morphology of the embedded particles and the overall film morphology.

Energy Dispersive X-ray Spectroscopy (EDS) revealed the highest concentration of fluorine (13%) on the surface sphere agglomerates of non-irradiated [C_2mim][fod]@PSU host–guest system. The presence of a very low amount of F on the surface of planar film (background), indicates that full blending of [C_2mim][fod] in PSU occurred in a very low extent, being mainly distributed on the surface as microcapsules (Table 1). Agglomerate surface composition indicates considerable amount of some type of $-SO_2$ subunit since de amount of S is notably higher (12.5%) than in pristine PSU (6.7%).

Apparently, light irradiation of the film promoted a deeper incorporation and higher compatibility between the host and the guest with low phase separation (Fig. 13a) and almost full incorporation (Fig. 13b). Upon irradiation at 290 nm, low values of F (3.7%) were found in the elongated protruding drop like particles on the surface (Fig. 13a), while in the matrix only 2.5% of F were detected. At higher wavelength irradiation (340 nm), only residual F levels were found (0.8%), while N, from $[C_2mim]^+$ cation was totally absent on the surface of both irradiated host–guest films (Table 1).

The distribution of each element in each sample was also analysed through elemental mapping.

At microscopic level, it became clear that appearance of the red colour on the film surface is concomitant with the improvement of film homogeneity (Fig. 13b).

Fig. 14 depicts fluorine and sulphur distribution, exclusively available in [C_2mim][fod] and PSU, respectively. Before irradiation both fluorine and sulphur are present in considerable higher amount in the droplet (sphere shape microstructure), which indicates the formation of strongly interaction between $-SO_2$ unit and [C_2mim][fod]. After irradiation at 290 nm, fluorine is considerably homogeneously dispersed on the film surface, with similar amount in both elongated droplet and film background, respectively 3.71 and 2.50%.

After irradiation at 340 nm all elements are homogeneously dispersed on the film surface, with residual amount of fluorine (1.30%) (Fig. S10, ESI†).

Fig. 15 show SEM elemental mapping of [C_2mim][BF_4]@PSU, that could be representative of a simpler host–guest system and could clarify the intriguing phenomena of increased emission after very short periods of light exposure. The outer surface showed porous structure with pore diameter ranging from 12 to 19 µm, which agrees with previously reported information.[29] Notably, immediately after confinement (before irradiation),

Table 1 Energy-dispersive X-ray spectroscopy (EDS) analysis of [C_2mim][fod]@PSU and [C_2mim][fod]@PSU after irradiation at 290 and 340 nm

	Element (%)			
[C_2mim][fod]@PSU	C (K)	O (K)	F (K)	S (K)
No irradiation				
Film background	73.73	15.78	1.30	8.89
Spherical droplet	33.80	3.70	13.10	12.50
290 nm irradiation				
Film background	67.60	17.20	2.50	8.0
Elongated droplet	65.8	15.2	3.71	9.4
340 nm irradiation				
Homogeneous film	69.5	13.9	1.30	8.92

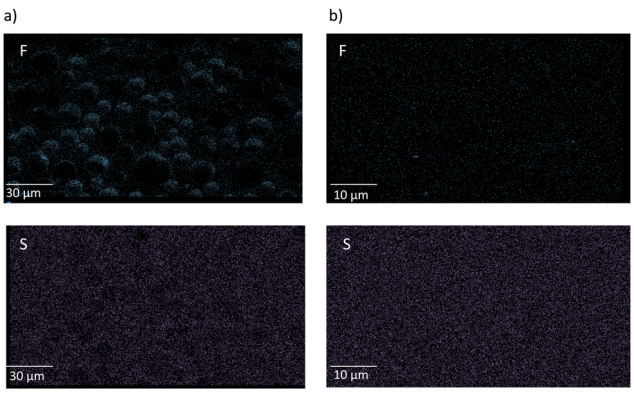

Fig. 14 Energy dispersive spectroscopy mapping of F and S of (a) [C_2mim][fod]@PSU and (b) [C_2mim][fod]@PSU irradiated at 290 nm.

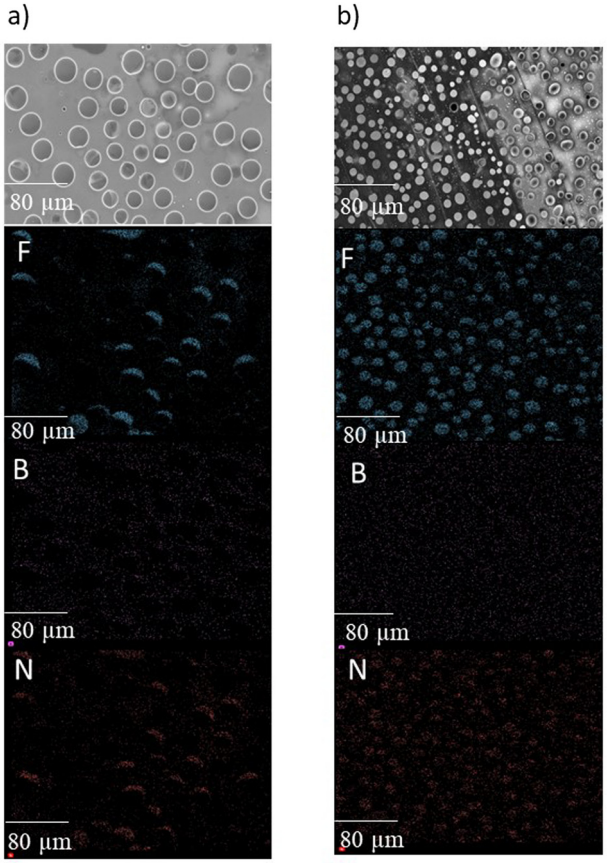

Fig. 15 Energy dispersive spectroscopy mapping of F, B and N of $[C_2mim]BF_4$@PSU (a) before and (b) after irradiation at 310 nm.

boron was found homogenously dispersed in the PSU surface. Apparently, irradiations seem to disintegrate the porous structures and expose its components, that are now agglomerated on the surface of polysulfone (Fig. 15b). It was previously reported that aromatic imidazolium ring interacts strongly with fluorine atoms from $[BF_4]^-$,[19,30] while boron is, apparently, uniformly distributed on the surface of the film even before 310 excitation of the film (Fig. 15). According with EDS results, the overall elemental concentration on the film surface was similar after irradiation. These observations point the possibility of promoting exposure of higher amount of emissive $[C_2mim][BF_4]$, that occur on the PSU surface during ILs immobilization, by using simple irradiation at a certain wavelength.

To clarify if fluorine, due to its high electron withdrawing character has some influence on the observed increased emission intensity after irradiation and pore fragmentation, the composite C_2mimCl@PSU, with no F in its composition was also evaluated in terms of emissive properties and surface morphology, before and after irradiation. Interestingly, and similarly to both $[C_2mim][BF_4]$@PSU and $[C_2mim][fod]$@PSU, the emissive profile of the doped film increased its emission intensity (Fig. 16a) at near 380 nm, while no significant morphological and elemental composition changes were observed on the film surface after irradiation at 314 nm (Fig. 16b and c).

Thermogravimetric analyses revealed that for $[C_2mim][fod]$@PSU, and as expected, the incorporated IL starts to degrade around 215 °C but the first step of degradation is longer and up to 280 °C indicating some degree of thermal protection from the PSU. Increasing the temperature, it is discernible a major step of degradation starting around 460 °C and ending at *ca.* 535 °C, corresponding to a mass loss 51.1%. The thermogravimetric curve profile is similar for the irradiated films, although a lower mass loss was observed between 250 and 500 °C, which may corroborate the suggested formation of different species originated from the embedded IL (Fig. S10, ESI†).

2.4 Water contact angle measurements

To determine the influence of irradiation on the wettability of the films, *i.e.*, their liquid absorption behaviour, water contact

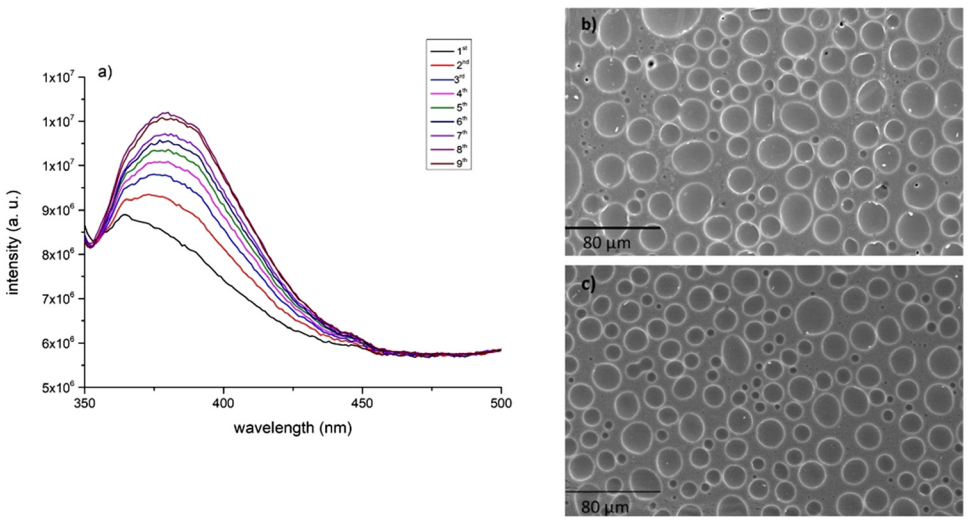

Fig. 16 (a) Emission spectra of C_2mimCl@PSU upon successive irradiations (1st–9th) at 314 nm (b) SEM images of C_2mimCl@PSU before irradiation (c) SEM images of C_2mimCl@PSU after irradiation at 314 nm.

Table 2 Water contact angles of (a) [C_2mim][fod]@PSU, (b) [C_2mim][fod]@PSU irradiated at 290 nm and (c) [C_2mim][fod]@PSU irradiated at 340 nm

	(a)	(b)	(c)
Water contact angle (°)	63 	69 	76 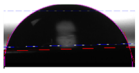

angle experiments were carried out at room temperature on the bottom surfaces of the irradiated and non-irradiated films.

The water contact angle established for [C_2mim][fod]@PSU (63°) revealed an hydrophilic surface, presenting a value lower than 90°. After irradiation at 290 nm the contact angle value increased to 69°, and the lower hydrophilic character, with a water contact angle of 76°, was found for the 340 nm irradiated film (Table 2).

These results are in accordance with the images obtained by Scanning Electron Microscopy, that suggest an incorporation of guests into the PSU host after irradiation, more pronounced at 340 nm. As aforementioned, we suggest that irradiation at 340 nm promotes an increased anion-cation interaction in both free and immobilized forms of [C_2mim][fod]. Hence, as consequence of the lower ionic character of the guest, that interaction results in a decrease of the hydrophilic character of the host–guest surface film.

3. Conclusion

We report here for the first time, a flexible polysulfone film doped with low amount of a photochromic highly fluorinated ionic liquid, that can detect UVA and distinguish UVA from UVB radiation.

Despite the interesting effect of UV irradiation on commercial imidazolium based ionic liquids, like [C_2mim][BF_4] and [C_2mim]Cl immobilized in polysulfone, the photophysical features that allow the doped PSU film to be used as a UVA/UVB differentiator must be attributed to the presence of the highly fluorinated β-diketonate anion, 1,1,1,2,2,3,3-heptafluoro-7,7-dimethyloctane-4,6-dionate. The very low intensity excitation band (300 nm) of PSU, reported here remains the only example of irradiation capable of increasing emissive properties of pristine and impregnated PSU films.

These results suggest that irradiation may promote incorporation of the host [C_2mim][fod] in the guest (PSU), more extensively when irradiated at the lower excitation wavelength.

We anticipate that host–guest systems based on polysulphone polymeric matrix will prove useful in fabricating highly sensitive UV sensors.

Is summary, [C_2mim][fod] dopped polysulfone film respond to UV exposure up to 370 nm, considerably above the 335 nm threshold of neat PSU, with the advantage of being detectable at naked eye when the irradiated area becomes red.

We are currently conducting further investigations to calibrate the here presented PSU dopped film to allow a direct readout of UV index equal to 7, value above which solar exposure becomes harmful.

Author contributions

B. Monteiro (investigation), J. P. Leal (investigation), M. Outis (formal analysis), M. H. Casimiro (formal analysis), C. C. L. Pereira (conceptualization, investigation, writing).

Conflicts of interest

There are no conflicts to declare.

Acknowledgements

This work was supported by the Associated Laboratory for Sustainable Chemistry-Clean Processes and Technologies-LAQV, which is financed by national funds from FCT/MEC (UID/QUI/50006/2019) and co-financed by the ERDF under the PT2020 Partnership Agreement (POCI-01-0145-FEDER–007265). The NMR spectrometers are part of The National NMR Facility, supported by Fundação para a Ciência e a Tecnologia (RECI/BBB-BQB/0230/2012). This work was also supported by Fundação para a Ciência e a Tecnologia (FCT) through the projects UIDB/00100/2020, and by Fundação para a Ciência e a Tecnologia through the contract no IST-ID/077/2018 (Bernardo Monteiro). Cláudia C. L. Pereira thanks Fundação para a Ciência e a Tecnologia, MCTES, for the Norma transitória DL 57/2016 Program Contract. Fundação para a Ciência e a Tecnologia I.P. for the national funds in the scope of the project UIDB/00100/2020.

References

1 E. Monroy, F. Calle, J. L. Pau, E. Muñoz, F. Omnès, B. Beaumona and P. Gibart, *J. Cryst. Growth*, 2001, **230**, 537–543.
2 E. Monroy, F. Omnès and F. Calle, *Semicond. Sci. Technol.*, 2003, **18**, R33–R51.
3 A. F. McKinlay and B. L. Diffey, *CIE J.*, 1987, **6**, 17–22.
4 International Commission on Illumination. *Erythema Reference Action Spectrum and Standard Erythema Dose*, CIE Central Bureau, Vienna, Austria, 1998. Commission Internationale de l'Eclairage (CIE) S007E-1998.
5 R. McKenzie, D. Smale and M. Kotkamp, *Photochem. Photobiol. Sci.*, 2004, **3**, 252–256.

6 M. Blumthaler, *Int. J. Environ. Res. Public Health*, 2018, **15**, 1723.
7 M. E. Lee and A. M. Armani, *ACS Sens.*, 2016, **1**, 1251–1255.
8 J. Wang, A. S. Jeevarathina, A. Jhunjhunwala, H. Ren, J. Lemaster, Y. Luo, D. P. Fenning, E. E. Fullerton and J. V. Jokerst, *Adv. Mater. Technol.*, 2018, **3**, 1800037.
9 H. Nakamura, H. Kitamura, N. Sato, M. Kanayama, Y. Shirakawa and S. Takahashi, *Nucl. Instrum. Methods Phys. Res., Sect. A*, 2015, **797**, 206–209.
10 A. Davis, G. H. W. Deane and B. L. Difey, *Nature*, 1976, **261**, 169–170.
11 G. Lindgren, B. L. Diffey and O. Larkö, *J. Ophthalmol.*, 1998, **82**, 1412–1415.
12 B. Diffey, *Atmosphere*, 2020, **11**, 125.
13 A. Henning, N. J. Downs and J. K. Vanos, *Int. J. Biometeorol.*, 2022, **66**, 627–640.
14 C. Gu, N. Hosono, J.-J. Zheng, Y. Sato, S. Kusaka, S. Sakaki and S. Kitagawa, *Science*, 2019, **363**, 387–391.
15 K. Mishra, N. Devi, S. S. Siwal, Q. Zhang, W. F. Alsanie, F. Scarpa and V. K. Thakur, *Adv. Sci.*, 2022, **9**, 2202187.
16 Y. Su, K. Otake, J.-J. Zheng, S. Horike, S. Kitagawa and C. Gu, *Nature*, 2022, **611**, 289–294.
17 B. Monteiro, M. Outis, H. Cruz, J. P. Leal, C. A. T. Laia and C. C. L. Pereira, *Chem. Commun.*, 2017, **53**, 850–853.
18 W. Tsang, D. R. Burgess Jr. and V. Babushok, *Combust. Sci. Technol.*, 1998, **139**, 385–402.
19 H. Nie, N. S. Schauser, N. D. Dolinski, J. Hu, C. J. Hawker, R. A. Segalman and J. Read de Alaniz, *Angew. Chem., Int. Ed.*, 2020, **59**, 5123.
20 R. Katoh, *Chem. Lett.*, 2007, **36**, 1256–1257.
21 Jacob M. Crosthwaite, Sudhir N. V. K. Aki, Edward J. Maginn and Joan F. Brennecke, *J. Phys. Chem. B*, 2004, **108**, 5113–5119.
22 S. Cha, T. Shim, Y. Ouchi and D. Kim, *J. Phys. Chem. B*, 2013, **117**, 10818–10825.
23 A. V. Parisi and M. G. Kimlin, *Photochem. Photobiol.*, 2004, **79**, 411–415.
24 V. Beghetto, V. Gatto, S. Conca, N. Bardella, C. Buranello, G. Gasparetto and R. Sole, *Carbohydr. Polym.*, 2020, **249**, 116810.
25 N. Takuya, G. Masako, K. Shigekazu and T. Kawai, *J. Am. Chem. Soc.*, 2008, **130**, 14570–14575.
26 E. Perju, L. Marin, V. C. Grigoras and M. Bruma, *Liq. Cryst.*, 2011, **38**, 893–905.
27 M. M. Farrukh, P. Bosch, M. Giagnorio, A. Tiraferri and M. Sangermano, *Polym. Int.*, 2017, **66**, 64–69.
28 A. L. Saroj, S. Krishnamoorthi and R. K. Singh, *J. Non-Cryst. Solids*, 2017, **473**, 87–95.
29 M. Farrokhara and F. Dorosti, *Chin. J. Chem. Eng.*, 2020, **28**, 2301–2311.
30 Y. Danten, M. I. Cabaço and M. Besnard, *J. Phys. Chem. A*, 2009, **113**, 2873–2889.